

PACS numbers: 42.55.Xi; 42.55.Rz; 42.65.An; 78.20.Nv
DOI: 10.1070/QE2009v039n12ABEH014160

Electronic and thermal lensing in diode end-pumped Yb : YAG laser rods and discs

O.L. Antipov, E.A. Anashkina, K.A. Fedorova

***Abstract*. The lensing effects in diode end-pumped Yb : YAG laser rods and discs are studied. Two mechanisms of refractive-index changes are taken into account, thermal and electronic (due to the difference between the excited- and ground-state Yb^{3+} polarisabilities), as well as pump-induced deformation of the laser crystal. Under pulsed pumping, the electronic lensing effect prevails over the thermal one in both rods and discs. In rods pumped by a highly focused cw beam, the dioptric power of the electronic lens exceeds that of the thermal lens, whereas in discs steady-state lensing is predominantly due to the thermal mechanism.**

Keywords: *thermal lensing, electronic lensing, Yb : YAG laser crystals, diode end-pumping, laser discs, laser rods.*

1. Introduction

Refractive-index changes induced in the active medium of solid-state lasers by intense pumping have a significant effect on the spatiotemporal and power characteristics of the output beam. Narrow-band diode pumping of laser crystals enables a reduction in thermalisation energy and, in addition to thermal lensing effects, which have been studied in sufficient detail (see e.g. Refs [1 – 8]), one must then take into account the electronic mechanism of index changes, associated with changes in the populations of activator-ion levels differing in polarisability [9, 10].

This work analyses electronic and thermal lensing in Yb : YAG discs and rods, in which 941-nm pumping minimises the thermal load (because of the small difference between the pump and lasing photon energies and because there is no excited-state absorption, up-conversion or cross-relaxation), and the contribution of the electronic mechanism of index changes to induced lensing effects may play an important role [9]. In examining electronic lensing, we rely on recent experimental data on the difference between the excited- and ground-state Yb^{3+} polarisabilities [9].

O.L. Antipov, E.A. Anashkina, K.A. Fedorova Institute of Applied Physics, Russian Academy of Sciences, ul. Ulyanova 46, 603950 Nizhnii Novgorod, Russia; e-mail: antipov@appl.sci-nnov.ru

Received 25 May 2009; revision received 3 August 2009
Kvantovaya Elektronika **39** (12) 1131 – 1136 (2009)
Translated by O.M. Tsarev

2. Basic mechanisms of lensing in Yb : YAG crystals

The pump-induced index change in an Yb : YAG crystal can be represented as the sum of electronic (δn_e) and thermal (δn_T) components [1 – 3, 9, 10]:

$$\delta n = \delta n_e + \delta n_T. \tag{1}$$

Since narrow-band pumping increases the population of only one long-lived state, $^2F_{5/2}$, the polarisability difference Δp between this state and the $^2F_{7/2}$ ground state determines the electronic contribution to the index change [9]:

$$\delta n_e = 2\pi F_L^2 n_0^{-1} \Delta p \delta N_2, \tag{2}$$

where $F_L = (n_0^2 + 2)/3$ is the Lorentz local-field factor; n_0 is the unaffected refractive index; and δN_2 is the change in the population of the $^2F_{5/2}$ upper laser level.

The upper-level population, N_2, can be found by solving (using the Runge – Kutta method) the following rate equation with a pump source term:

$$\frac{\partial N_2}{\partial t} + \frac{N_2}{\tau_{21}} + \frac{\gamma_{ASE}}{\tau_{21}} N_2^2 = \frac{\sigma_{03} N_0}{h\nu_{03}} I(r, z, t), \tag{3}$$

where σ_{03} is the pump absorption cross section; τ_{21} is the upper-level lifetime; N_0 is the ground-state population; $N_0 + N_2 \approx N_\Sigma = \text{const}$; N_Σ is the total activator ion concentration; h is the Planck constant; ν_{03} is the pump frequency; $I(r, z, t)$ is the pump intensity distribution in the laser crystal; and γ_{ASE} characterises the low-gain amplified spontaneous emission intensity [4, 11]. For rods, γ_{ASE} can be estimated as $\sim {}^1/_4 \pi \sigma_{21} a^2 L^{-1}$ (where σ_{21} is the laser transition cross section; L is the sample length; and a is the pump beam radius); for discs, $\gamma_{ASE} \approx {}^1/_2 \pi \sigma_{21} L$ (for a pump beam diameter far exceeding the disc thickness). Luminescence reduces the effective upper level lifetime, $\tau_{eff} = \tau_{21} \times (1 + \gamma_{ASE} N_2)^{-1}$, thereby influencing the lensing dynamics and strength [4].

The thermal component of the index change can be represented in the form [1 – 3]

$$\delta n_T = \frac{\partial n}{\partial T} \delta T + \delta n_{ph} = \left(\frac{\partial n}{\partial T} + 2 n_0^3 \alpha_T C \right) \delta T, \tag{4}$$

where $(\partial n/\partial T)\delta T$ is the index change due to the temperature variation of resonance frequencies; δn_{ph} represents the

photoelastic effect [1, 2]; C is the polarisation-averaged photoelastic constant [2]; and α_T is the linear thermal expansion coefficient. The temperature change δT was found by solving the following heat equation with heat sources representing the pump energy thermalisation through nonradiative transitions:

$$\rho c_p \frac{\partial T}{\partial t} - K\Delta T = h\nu_{32} N_3 w_{32} + h\nu_{10} N_1 w_{10}, \tag{5}$$

where K is thermal conductivity; ρ is density; c_p is the specific heat of the crystal at constant pressure; ν_{32} and w_{32} are the frequency and rate of the nonradiative transition from the pump level (3) to the upper laser level (2); N_3 is the population of level 3; ν_{10} and w_{10} are the frequency and rate of the nonradiative transition from the lower laser level to the ground state; and N_1 is the population of the lower level.

The heat sources in Eqn (5) were evaluated from rate equations under the assumption that the nonradiative relaxation times are much shorter than τ_{21}:

$$N_3 w_{32} \approx \frac{\sigma_{03} N_0}{h\nu_{03}} I(r, z, t), \tag{6}$$

$$N_1 w_{10} \approx \gamma_{\mathrm{ASE}} N_2^2 + \frac{N_2}{\tau_{21}}. \tag{7}$$

We also assumed the heat in the rod to be removed through its lateral surface (thermally isolated ends), and that in the disc, through one of its faces (with the other face and lateral surface thermally isolated). In both cases, the cooled surfaces were subject to the third-order boundary condition [2, 3, 12]

$$K\nabla_\xi T + H(T - T_0) = 0, \tag{8}$$

where T_0 is the temperature of the (copper) heatsink; ∇_ξ is a derivative along the normal to the cooled surface; and H is the heat transfer coefficient. Typical H values for the YAG–Cu interface are 0.5 to 2 W cm^{-2} K^{-1}, depending on the quality and composition of the contact layer [3]. Equation (5) with the boundary condition (8) was solved numerically by the finite-difference method.

The thermal stress and strain in rods and discs were assessed by solving a quasi-static thermoelastic problem for a particular temperature field. The Yb:YAG crystal was taken to be isotropic, with Young's modulus E and Poisson's ratio ν. The problem was formulated in terms of stresses, and strain compatibility equations were used [13]. The results allowed us to evaluate the contribution of rod/disc shape changes to thermal lensing and to compare the maximum thermal stress to the strength of YAG crystals.

The change in optical pathlength $\delta(r, z)$ over length $\mathrm{d}z$ along the crystal axis, with an accuracy to the second-order infinitesimals, is given by [1]

$$\delta(r, z) = \mathrm{d}z[\delta n + (n_0 - 1)\varepsilon_{zz}], \tag{9}$$

where ε_{zz} is the component of the strain tensor, ε_{ij}. The term $\mathrm{d}z(n_0 - 1)\varepsilon_{zz}$ in (9) represents the elongation of a volume element (the optical pathlength increases in the crystal but decreases in the air).

In the paraxial approximation (the diameter of the amplified beam is smaller than that of the pump beam), the dioptric lens power is given by D,

$$D = 2 \left.\frac{\partial \Delta}{\partial r^2}\right|_{r=0}, \tag{10}$$

where Δ is the optical path difference between the on-axis pump ray and a parallel ray at a distance r from the axis:

$$\Delta = \int_0^L [\delta(0, z) - \delta(r, z)]\mathrm{d}z. \tag{11}$$

The dioptric powers of the electronic (D_e) and thermal (D_T) lenses can then be written in the form

$$D_\mathrm{e} = 2 \frac{2\pi F_\mathrm{L}^2 \Delta p}{n_0} \frac{\partial}{\partial r^2} \times \left\{ \int_0^L [N_2(0, z, t) - N_2(r, z, t)]\mathrm{d}z \right\} \Bigg|_{r=0}. \tag{12}$$

$$D_T = 2\left(\frac{\mathrm{d}n}{\mathrm{d}T}\right)_\mathrm{eff} \frac{\partial}{\partial r^2} \left\{ \int_0^L [T(0, z, t) - T(r, z, t)]\mathrm{d}z \right\} \Bigg|_{r=0}, \tag{13}$$

where $(\mathrm{d}n/\mathrm{d}T)_\mathrm{eff}$ is the effective thermooptical coefficient, which takes into account $\partial n/\partial T$, the thermal expansion of the sample, and the photoelastic effect.

The maximum stress in discs ($\sigma_\mathrm{max}^\mathrm{disk}$) and rods ($\sigma_\mathrm{max}^\mathrm{rod}$) was evaluated in the plane-stress and plane-strain approximations, respectively [13]:

$$\sigma_\mathrm{max}^\mathrm{disk} \approx \sqrt{2}\, \frac{\alpha_T E}{4} \Delta T_\mathrm{max}, \tag{14}$$

$$\sigma_\mathrm{max}^\mathrm{rod} \approx \sqrt{2}\, \frac{\alpha_T E}{4(1 - \nu)} \Delta T_\mathrm{max}, \tag{15}$$

where ΔT_max is the maximum temperature difference in the radial direction of the crystal. The Yb:YAG parameters used in our computations are given below.

Polarisability difference between the upper laser level ($^2\mathrm{F}_{5/2}$) and the ground level ($^2\mathrm{F}_{7/2}$) at 633 nm, $\Delta p/\mathrm{cm}^3$ ..... 2×10^{-26} [9]
Refractive index, n_0 ..... 1.82 [3]
Pump frequency, $\nu_{03}/\mathrm{cm}^{-1}$ ..... 10624 [3]
Frequency of the transition from the pump level to the upper laser level, $\nu_{32}/\mathrm{cm}^{-1}$ ..... 297 [3]
Frequency of the transition from the lower laser level to the ground state, $\nu_{10}/\mathrm{cm}^{-1}$ ..... 612 [3]
Pump absorption cross section, $\sigma_{03}/\mathrm{cm}^2$ ..... 7.7×10^{-20} [3]
Laser transition cross section, $\sigma_{21}/\mathrm{cm}^2$ ..... 2.1×10^{-20} [3]
Upper-level lifetime, $\tau_{21}/\mu\mathrm{s}$ ..... 951 [3]
Thermooptical coefficient, $\partial n/\partial T/\mathrm{K}^{-1}$ ..... 7.3×10^{-6} [3]
Effective thermooptical coefficient (for rods) $(\mathrm{d}n/\mathrm{d}T)_\mathrm{eff}/\mathrm{K}^{-1}$ ..... 10^{-5} [2]
Density, $\rho/\mathrm{g\ cm}^{-3}$ ..... 4.56 [3]
Specific heat at constant pressure, $c_p/\mathrm{J\ g}^{-1}\ \mathrm{K}^{-1}$ ..... 0.59 [3]
Thermal conductivity, $K/\mathrm{W\ cm}^{-1}\ \mathrm{K}^{-1}$ ..... 0.14 [3]
Linear thermal expansion coefficient, α_T/K^{-1} ..... 7.5×10^{-6} [3]
Young's modulus, $E/\mathrm{kg\ cm}^{-2}$ ..... 3.1×10^7 [3]
Poisson's ratio, ν ..... 0.3 [3]
Tensile strength/kg cm^{-2} ..... 2×10^4 [3]

Photoelastic constants (plane-stress state):

C_r . . . . . 0.0032 [2]

C_θ . . . . . −0.011 [2]

Yb^{3+} concentration in the YAG crystal

(1% doping level), N_Σ/cm^{-3} . . . . . 1.38×10^{20} [3]

Substituting these parameters into (14) and (15), we obtain that the rod fractures at $\Delta T_{max} = 170$ K, and the disc at $\Delta T_{max} = 240$ K. In experiments, fracture may occur at lower temperature gradients because of the anchorage stress and structural defects [3].

3. Lensing in rods

We considered a multimode Gaussian pump beam and took into account its divergence in the rod, with a beam quality factor $M^2 \gg 1$ [2, 3]. The input beam width was taken to be much smaller than the pump absorption depth, and only the radial heat flow was considered. In this approximation, the heat equation is one-dimensional (in terms of r), and the z coordinate appears as a parameter in the right-hand side of (5).

Under low-intensity cw pumping (no absorption saturation and no luminescence), the upper-level population is proportional to the pump intensity, and the power of a steady-state electronic lens can be estimated from (12):

$$D_e = 2\,\frac{2\pi F_L^2 \Delta p}{n_0}\,\frac{P\tau_{21}}{\pi h \nu_{03}} \int_0^L \frac{\exp(-\alpha z)}{a^4(z)}\,dz, \qquad (16)$$

where P is the input pump power and $\alpha = \sigma_{03} N_\Sigma$ is the unsaturated pump absorption coefficient. The power of the thermal lens under the same conditions is given by

$$D_T = 2\left(\frac{dn}{dT}\right)_{eff} \frac{\nu_{32} + \nu_{10}}{\nu_{03}}\,\frac{\alpha P}{4\pi K} \int_0^L \frac{\exp(-\alpha z)}{a^2(z)}\,dz. \qquad (17)$$

It follows from (16) and (17) that, at a constant pump beam radius, a_0, the power of the thermal lens is proportional to a_0^{-2}, and that of the electronic lens, to a_0^{-4}. Therefore, with decreasing a_0 the power of the electronic lens rises more rapidly than that of the thermal lens, whereas at a considerable beam width the total lensing effect is dominated by the thermal component.

Our computation results [in the complete model represented by Eqns (2)–(13)] indicate that, in the case of a highly focused pump beam, the absorption saturation, population inversion decay through luminescence, and the strong beam convergence over the length of the rod reduce the powers of the two lenses and alter their dependence on the pump beam width (the ratio of the electronic and thermal lens powers is no longer proportional to a_0^{-2}), but the electronic lensing effect remains stronger than the thermal one (Fig. 1a). At a pump beam diameter above 400 μm, the thermal lensing effect prevails, in good agreement with thermal lensing estimates and measurements [2, 3].

In analysing the pulsed regime, we considered a single rectangular pulse of duration τ_p, comparable to the electronic lensing relaxation time, τ_{eff}. Our computations demonstrate that, independent of the pump beam diameter, the electronic lensing effect prevails over the thermal one (Fig. 1b). This can be rationalised in terms of a simplified model. At a short pump pulse duration, $\tau_p \ll \tau_T$ [where $\tau_T \approx a_0^2/(4\chi)$ is the thermal relaxation time on the length scale of the pump beam radius and $\chi = K/(\rho c_p)$ is thermal diffusivity], the derivatives with respect to r in Eqn (5) can be neglected in comparison with the time derivative. Then, in the absence of absorption saturation and luminescence, the power of the thermal lens can be found by substituting the temperature field into (13):

$$D_T = 2\left(\frac{dn}{dT}\right)_{eff} \frac{\alpha P}{\pi c \rho} \left\{ \frac{\nu_{32} + \nu_{10}}{\nu_{03}}\, t - \frac{\nu_{10}}{\nu_{03}}\,\tau_{21} \times \left[1 - \exp\left(-\frac{t}{\tau_{21}}\right)\right]\right\} \int_0^L \frac{\exp(-\alpha z)}{a^4(z)}\,dz. \qquad (18)$$

The rate equation (3) (with $\gamma_{ASE} = 0$ and $N_0 \approx N_\Sigma$) can be integrated. As a result, using (12) we find the power of the electronic lens:

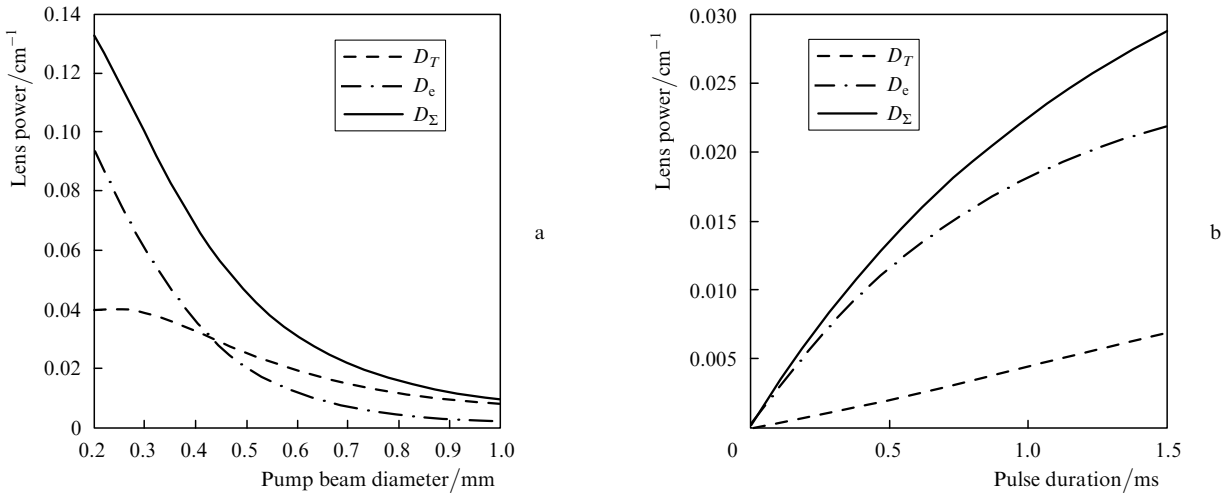

Figure 1. Induced-lens power as a function of (a) cw pump beam diameter (20-W power) and (b) pump pulse duration (40-W peak power, 600-μm focal spot) for a 2 % Yb : YAG rod 15 mm in length and 2 mm in diameter: electronic (dot-dashed curves), thermal (dashed curves) and total (solid curves) lensing effects.

$$D_e = \frac{4\pi F_L^2 \Delta p}{n_0} \frac{P\tau_{21}}{\pi h \nu_{03}} \left[1 - \exp\left(-\frac{t}{\tau_{21}}\right)\right] \int_0^L \frac{\exp(-\alpha z)}{a^4(z)}\, dz. \quad (19)$$

In this approach, the lens powers vary similarly ($\sim a_0^{-4}$) with pump beam diameter but differ in rise time behaviour.

4. Lensing in discs

The mechanical stress in an anchored disc deforms it, leading to distortion of the probe beam phase front even in the absence of pumping [4, 5]. Pumping contributes to the lensing effect, as examined below.

We considered a disc with a mirror on its face at $z = L$, pumped by a collimated high-power Gaussian beam through the face at $z = 0$. At a beam radius considerably greater than the disc thickness, $a_0 \gg L$, there is only axial heat flow. The thermoelastic problem was solved in the plane-stress approximation with two types of boundary conditions: the mirrored face free or fixed. We assumed that deformation of the disc did not disturb the heat removal and neglected the effect of tension on bending. The problems of thermal expansion and bending were treated independently [14]. In this model, the thermal lensing component related to the thermooptical coefficient can be written in the form [2]

$$D_T = 4\left[\frac{\partial n}{\partial T} + 2n_0^3 \alpha_T C + \alpha_T (n_0 - 1)(1 + \nu)\right] \times \frac{\partial}{\partial r^2}\left\{\int_0^L [T(0, z, t) - T(r, z, t)]dz\right\}\Big|_{r=0}, \quad (20)$$

where the third term in square brackets represents thermal expansion. Since the lens power in the disc was evaluated for two passes of the probe beam, the thermal lensing component of D_T in (20) unrelated to bending and the electronic-lens power differ from those for rods in (13) and (12) by a factor of 2.

The temperature difference across the disc [$T(z = 0) > T(z = L)$] causes it to bend (Fig. 2), and the deformed (convex) mirror on its face defocuses the probe beam. This lensing effect (of dioptric power D_m) is missing in rods. The problem of disc bending was treated using the theory of small bending of thin circular plates [13]. The solution translates to the following expression for the curvature of mirror (at $r = 0$ along the z axis):

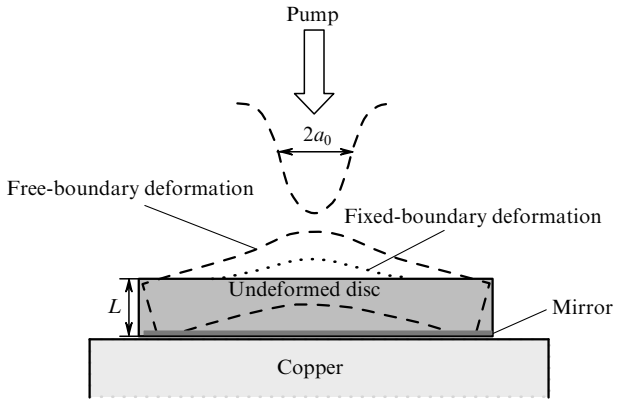

Figure 2. Pump-induced deformation of a laser disc.

$$k_r = \frac{(1 + \nu)k_T}{2}, \quad (21)$$

where

$$k_T = \frac{12\alpha_T}{L^3} \int_0^L T(0, z, t)\left(z - \frac{L}{2}\right)dz \quad (22)$$

with time as a parameter. From (21) and (22), we can estimate the two-pass dioptric lens power ($D_m = 2k_r$) related to the mirror bending on the face at $z = L$. The induced-lens power in the disc can be represented as the sum of three terms, one representing the electronic lensing, and the other two representing the thermal lensing:

$$D_\Sigma = D_e + D_T + D_m. \quad (23)$$

In the case of free boundaries, the bending-induced component D_m varies with pump beam width in a different way from D_T and D_e: neglecting the luminescence and absorption saturation, we have $D_m \sim a_0^{-2}$, whereas D_e and D_T vary as $\sim a_0^{-4}$. The total lensing effect may be both positive and negative, depending on the parameters of the system. With the mirror fixed (no bending, $D_m = 0$), the total lensing effect is always focusing.

Under cw pumping, the power of the thermal lens, D_T, depends on the heat transfer coefficient, H: the better the heat removal, the lower the value of D_T. The power of the bending component, D_m, is independent of H and is determined by the z-axis temperature gradient (at $r = 0$).

Numerical and analytical evaluation of the terms in (26) demonstrates that, under cw pumping, the thermal lensing effect is stronger than the electronic one (Fig. 3), in good agreement with induced-lensing measurements in Yb : YAG discs [4, 5] and theoretical estimates [6, 8].

Under pulsed pumping, the lensing effect is weak and (for $\tau_p \leqslant \tau_{21}$) the power of the electronic lens, D_e, exceeds that of the thermal lens, D_T (Fig. 4). Increasing the number of pump passes across the active medium (or increasing the Yb^{3+} concentration) increases the power of the lenses, but the relationship between them varies little. At short pulse durations, $\tau_p \ll \tau_T$ ($\tau_T \approx L^2/\chi$ for discs), the powers of the thermal and electronic lenses vary with time in the same way as in the case of rods [relations (18) and (19), respectively]. Under intense pumping, the electronic lensing effect develops more rapidly (Figs 4a, 4b), which is due to the shorter effective upper-level lifetime because of the amplified spontaneous emission [4]. Index change measurements under pulsed pumping [9] confirm that the electronic component makes a significant contribution to the total lensing effect.

Note that, under pulsed pumping, the electronic lensing effect may be stronger than the thermal one (related to the thermooptical coefficient) in both Yb : YAG and other laser crystals of various geometries [14].

5. Conclusions

Theoretical analysis and numerical simulation indicate that the induced lensing effect in diode end-pumped Yb : YAG laser crystals comprises several components: the refractive-index changes caused by local electronic and nonlocal thermal mechanisms and the changes in the shape and reflectance of the crystal due to thermal stresses. The

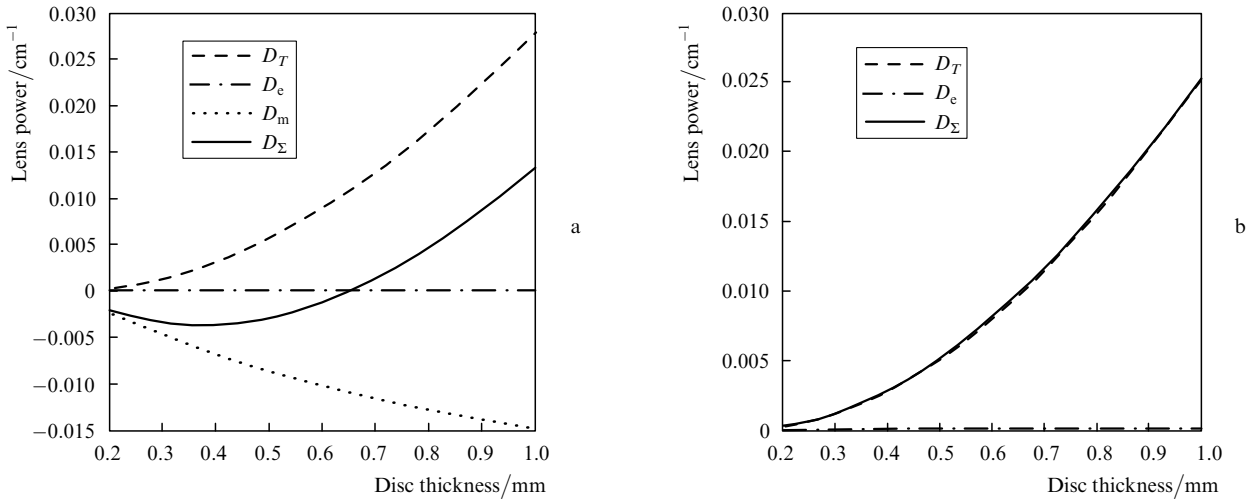

Figure 3. Induced-lens power as a function of disc thickness for a 9 % Yb : YAG disc at a pump power of 1 kW and pump beam diameter of 5 mm: (a) fixed boundary, (b) free boundary; electronic lensing (dot-dashed curves), thermal lensing related to the thermooptical coefficient (dashed curves), bending-induced thermal lensing (dotted curve) and total effect (solid curves).

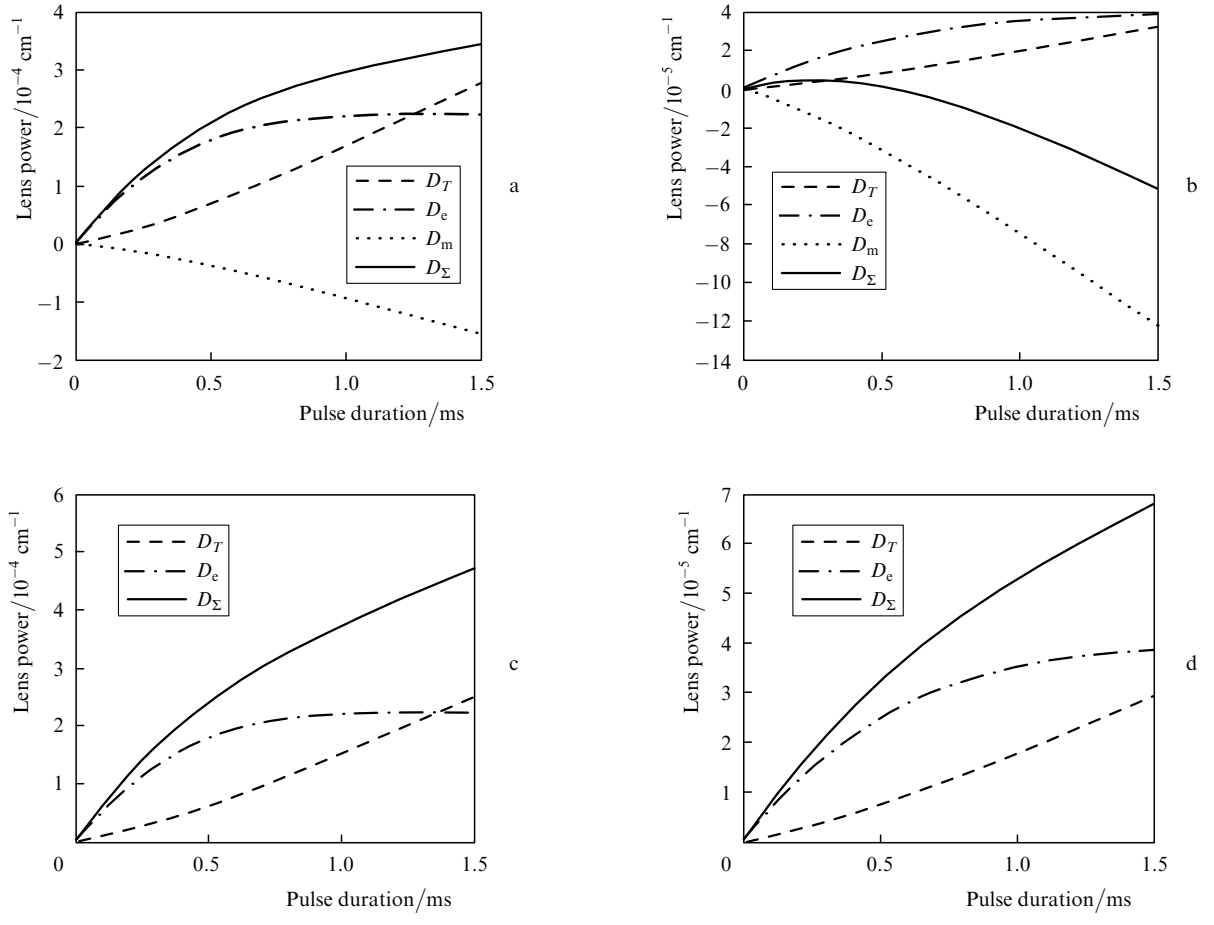

Figure 4. Induced-lens power as a function of pump pulse duration (1-kW power) for 9 % Yb : YAG discs: (a) free boundary, 600-μm-thick disc, 4-mm-diameter pump beam; (b) free boundary, 300-μm-thick disc, 6-mm-diameter pump beam; (c) fixed boundary, 600-μm-thick disc, 4-mm-diameter pump beam; (d) fixed boundary, 300-μm-thick disc, 6-mm-diameter pump beam; electronic lensing (dot-dashed curves), thermal lensing related to the thermooptical coefficient (dashed curves), bending-induced thermal lensing (dotted curves) and total effect (solid curves).

induced lensing in discs may be both positive and negative, depending on the disc thickness and pump beam width, whereas that in rods is always positive.

Electronic lensing in pulse-pumped Yb : YAG rods and discs must be taken into account together with thermal lensing. The same refers to rods pumped with a highly focused cw pump beam. Under cw pumping, the thermal lensing effect prevails in discs and also in rods at large beam diameters. Changes in the shape of the disc make an appreciable contribution to the induced lensing, whereas

the distortion of the probe beam phase front in long rods is determined by index changes rather by deformation of their faces.

Note that the electronic lensing effect will be weaker in amplifiers and oscillators upon a marked homogeneous reduction in excited-state population (e.g., under gain saturation conditions) throughout the pumped region of the crystal. The power of the thermal lens may then increase owing to the higher heat release rate. At the same time, a mismatch between the inversion and amplification regions due to the competition between the electronic and thermal mechanisms may cause further spatial distortion of the refractive index. Electronic lensing is a rather universal effect and would be expected to occur as well in other laser crystals doped with Yb^{3+} (or other rare-earth or transition-metal ions).

Acknowledgements. This work was supported by the Russian Foundation for Basic Research (Grant No. 07-02-92184-NTsNI_a) and the Physical Sciences Division of the Russian Academy of Sciences (Nonlinear Optics of Unique Laser Systems Programme).

References

1. Mezenov A.V., Soms L.N., Stepanov A.I. *Termooptika tverdotel'nykh lazerov* (Thermooptics of Solid-State Lasers) (Leningrad: Mashinostroenie, 1986).
2. Chenais S., Druon F., Forget S., Balembois F., Georges P. *Prog. Quantum Electron.*, **30**, 89 (2006).
3. Koechner W. *Solid-State Laser Engineering* (New York, Springer Science + Business Media, 2006).
4. Antognini A., Schuhmann K., Amaro F.D., Biraben F., Dax A., Giesen A., Graf T., Hänsch T.W., Indelicato P., Julien L., Kao C.-Y., Knowles P.E., Kottmann F., Le Bigot E., Liu Y.-W., Ludhova L., Moschüring N., Mulhauser F., Nebel T., Nez F., Rabinowitz P., Schwob C., Taqqu D., Pohl R. *IEEE J. Quantum Electron.*, **45**, 983 (2009).
5. Stewen C., Contag K., Larionov M., Giesen A., Hügel H. *IEEE J. Sel. Top. Quantum Electron.*, **6**, 650 (2000).
6. Garnov S.V., Mikhailov V.A., Serov R.V., Smirnov V.A., Tsvetkov V.B., Shcherbakov I.A. *Kvantovaya Elektron.*, **37**, 910 (2007) [*Quantum Electron.*, **37**, 910 (2007)].
7. Bogdanov Yu.V., Papchenko A.A., Sorokin V.N. *Kvantovaya Elektron.*, **21**, 1041 (1994) [*Quantum Electron.*, **24**, 968 (1994)].
8. Snetkov I.L., Solov'ev A.A., Khazanov E.A. *Kvantovaya Elektron.*, **39**, 302 (2009) [*Quantum Electron.*, **39**, 302 (2009)].
9. Antipov O.L., Bredikhin D.V., Eremeikin O.N., Ivakin E.V., Savikin A.P., Sukhodolov A.V., Fedorova K.A. *Kvantovaya Elektron.*, **36**, 418 (2006) [*Quantum Electron.*, **36**, 418 (2006)].
10. Ivakin E.V., Sukhadolau A.V., Antipov O.L., Kuleshov N.V. *Appl. Phys. B*, **86**, 315 (2007).
11. Svelto O. *Principles of Lasers* (New York: Plenum, 1982; Moscow: Mir, 1990).
12. Carslaw, H.S., Jaeger, J.C. *Conduction of Heat in Solids* (Oxford: Clarendon, 1959; Moscow: Nauka, 1964).
13. Kovalenko A.D. *Osnovy termouprugosti* (Fundamentals of Thermoelasticity) (Kiev: Naukova Dumka, 1970).
14. Planchon T.A., Amir W., Childress C., Squier J.A., Durfee C.G. *Opt. Express*, **16**, 18557 (2008).